

NASA-CR-168172  
19840010254

NASA-CR-168,172

NASA CR-168172



SPUTTERING PHENOMENA IN ION THRUSTERS

PREPARED FOR  
LEWIS RESEARCH CENTER  
NATIONAL AERONAUTICS AND SPACE ADMINISTRATION  
GRANT NAG 3-209

**LIBRARY COPY**

APR 1984

LANGLEY RESEARCH CENTER  
LIBRARY NASA  
HAMPTON, VIRGINIA

Final Report

February 1983

Raymond S. Robinson and Stephen M. Rossnagel

Department of Physics  
Colorado State University  
Fort Collins, Colorado 80523



NF02599

TABLE OF CONTENTS

I.	INTRODUCTION . . . . .	1
II.	ION THRUSTER DISCHARGE CHAMBER SIMULATION SETUP . . . . .	4
III.	DUAL ION BEAM SYSTEM . . . . .	7
IV.	STRESS AND ITS MEASUREMENT IN FILMS . . . . .	12
V.	PROCEDURE AND RESULTS . . . . .	17
	A. Films Inside a Thruster . . . . .	17
	B. Film Formation in a Dual Ion Beam System . . . . .	22
VI.	CONCLUSIONS . . . . .	26
	REFERENCES . . . . .	28
	APPENDIX . . . . .	30

## I. INTRODUCTION

Electrostatic ion thrusters have been undergoing intensive development and basic research for some time. The first electrostatic thruster was tested in 1960.<sup>1</sup> As the technology has developed, the stringent requirements for long lifetimes (thousands to tens of thousands of hours) with unattended operation have been a governing factor in component design. A 30-cm mercury ion thrust subsystem is now available for primary propulsion applications.<sup>2</sup> An 8-cm mercury ion thrust subsystem has also been developed for auxiliary propulsion and is available for applications such as station keeping and attitude control.<sup>3</sup>

Sputtering effects can be lifetime limiting for ion thrusters in basically two ways: (1) ion bombardment of critical thruster components at energies sufficient to cause sputtering can remove significant quantities of material; enough to degrade operation through adverse dimensional changes or possibly lead to complete component failure, and (2) metals sputtered from these intensely bombarded components can be deposited in other locations as thin films and subsequently flake or peel off; the flakes then lodging elsewhere in the discharge chamber with the possibility of providing conductive paths for short circuiting of thruster components such as the ion optics.

Processes limiting ion thruster operational lifetime continue to be of vital interest to both the designer and user of electrostatic propulsion. Sputter erosion of the screen electrode in the ion optics system has been treated in detail by Beattie.<sup>4</sup> Sputtering was the most probable cause of high voltage shorts encountered in the SERT II flight test.<sup>5</sup> High voltage shorts and ion optics damage were caused by metal flakes in a 10,000 hour endurance test of a 30-cm mercury ion thruster.<sup>6,7</sup>

An accelerated life test of a small (5-cm) mercury ion thruster showed that appropriate surface preparation techniques and choices of materials used in the discharge chamber could reduce the problems of sputtered deposit peeling and flaking.<sup>8,9</sup> Studies of methods for eliminating or reducing the effects of internal erosion in a 30-cm mercury thruster have been fairly successful from the standpoint of increased operating lifetime.<sup>10</sup> The problem of peeling of metallic flakes and the subsequent movement of flakes within the discharge chamber is probably the more difficult to overcome because of its present unpredictability. Some work has gone into the problem of clearing high voltage shorts caused by chips or flakes;<sup>11</sup> however, discharging a capacitor through the grids to vaporize a chip is also potentially hazardous to high permeance optics. Peeling and flaking problems occur on a different time scale in actual space operation than in some ground-based simulations because, as shown by Rawlin and Mantenieks,<sup>12</sup> even small quantities of background nitrogen gas in ground test facilities greatly reduce erosion rates of thruster components; this was also studied in detail by Wilbur<sup>13</sup> and Masaki.<sup>14</sup>

Intrinsic stress in deposited films is an important parameter when failure and peeling of films is considered. Simultaneous ion bombardment of a growing film has been shown to have a significant effect on the intrinsic stress and bonding in thin films;<sup>15,16</sup> in some cases, modifying the stress sufficiently to change from compressive to tensile stress simply by varying the parameters of the bombarding ion beam.<sup>17</sup> Other possible interactions include the preferential sputtering of various impurity species, such as oxygen and carbon, which may possibly be present in a growing film. In a discharge chamber, surfaces at

different applied potentials will receive ion fluxes that vary in energy with the more negative surfaces being bombarded by higher energy ions. Thus, deposited film properties as well as sputter etch rates should be different for various components and surfaces in a discharge chamber. The angle of incidence of arriving material and background gas pressure have also been shown to alter and sometimes change the sign of the stress of Mo, Ta, and stainless steel films.<sup>18</sup>

This work has concentrated in two areas. The first has been to operate thrusters for multi-hour periods and to observe and measure the films found inside the thruster. The second has been to simulate the environment inside the discharge chamber of the thruster by means of a dual ion beam system. Here, films were sputter deposited in the presence of a second low energy bombarding beam to simulate film deposition on thruster interior surfaces that undergo simultaneous sputtering and deposition.

## II. ION THRUSTER DISCHARGE CHAMBER SIMULATION SETUP

One of the two primary experimental simulations in this study was to observe film characteristics inside actual operating thrusters. For this purpose, a 15-cm diameter multipole thruster was set up to operate in a 45-cm diameter vacuum system. The vacuum system had as its primary vacuum pump a 6" diffusion pump and is also equipped with a liquid nitrogen trap. The base pressure in this system was in the  $1 \times 10^{-7}$  Torr range. The power supplies were arranged to provide for a fairly realistic thruster operating range.

The thruster was of multiple design, having four annular anodes, and five accompanying annular pole pieces. The back plate was flat with no anodes. Thermionic Ta filament cathodes were used to provide primary electrons for the discharge. The cathodes were mounted on posts extending from the back plate. Ion optics were Mo dished grids with hole diameters of 2.0 mm for both the screen and accelerator grids and center to center aperture spacings of 2.5 mm. The grid separation was fixed to approximately 1.5 mm. Aside from the Mo grids and Ta cathode filaments, all other thruster parts were stainless steel except for the soft iron pole pieces and the Alnico V permanent magnets.

To prepare the interior surfaces of the thruster, each metal piece was sanded to a shiny metal finish. Final sanding was done using 600 grit paper. The parts that could not be sanded such as alumina insulators were thoroughly cleaned and acid etched. All parts were then ultrasonically cleaned inalconox, rinsed in large amounts of hot  $H_2O$ , and baked for several hours prior to assembly. Assembly was accomplished using gloves under clean room conditions.

Argon was used as the propellant gas. The leak valve was connected through tubing to openings in the back plate of the thruster. Typical operating pressures of the vacuum system were  $1 \times 10^{-4}$  Torr at a flow rate of 1-2 sccm of Ar.

In many laboratory-based ion thrusters, films are often formed on the back plate of the discharge chamber. This is partly due to physical sputtering of objects in the ion beam downstream from the thruster. Sputtered material then returns through the relatively large open area of the grids and deposits inside the thruster, thus masking purely discharge chamber effects that would be present during operation on a spacecraft. To alleviate this problem, an attempt was made to decelerate the ion beam prior to striking a target. If the ion energy could be reduced to less than the sputtering threshold (30-50 eV for most materials) then physical sputtering would be eliminated and redeposition inside the source reduced. Deceleration of the beam was attempted by placing a grounded stainless steel screen normal to the beam  $\geq 20$  cm from the accelerator grid. Approximately 2-3 mm downstream of the screen, a conducting plate was placed parallel to the screen and biased positively to almost beam voltage. However, due to the relatively large screen-plate distance, and the increase of the plasma potential of the beam along with the target bias, this method proved ineffective. This method did result in somewhat reduced sputtering of the target, but also caused increased sputtering of the downstream side of the accelerator grid. In practice, to reduce the effect of back-sputtering, the beam voltage was simply kept low without using any beam deceleration.

Upon reassembly, the thruster was mounted in the vacuum chamber and operated for several days to determine an operating baseline.

Typically, the discharge was set in the range of 40-75 eV at 0.4 to 4 Amps total. The beam voltage was kept low, at  $< 100$  eV, to minimize the amount of facility back-sputtered material entering the discharge chamber. Beam currents then were also low,  $\sim 60$ -100 mA, which for a 15 cm diameter thruster was in the range of  $\sim 0.2$ -0.5 mA/cm<sup>2</sup>. The accelerator grid was typically -70 to -100 V and the impingement current  $\sim 10\%$  of the total beam current partly due to poor focusing and partly due to operation at  $1 \times 10^{-4}$  Torr. Neutralization was accomplished using a thermionic Ta filament.

Test samples of various types (to be discussed below) were then mounted at different positions inside the thruster discharge chamber. The thruster was then operated for a fixed period of time, usually 7-8 hours, under various operating conditions. The samples were then removed and examined for film deposition, film composition, and residual stresses in the film. These results will be discussed below.

### III. DUAL ION BEAM SYSTEM

In contrast to the experiments with film growth in operating thrusters, experiments were performed with a dual-ion beam system to produce and modify films outside the thruster body. In this dual ion beam system, one beam is directed at a target made of some relevant thruster material, such as molybdenum. The Mo atoms sputtered from this target emerge from the surface in roughly a cosine distribution; normal to the surface being  $0^\circ$ . Upon striking other surfaces, these Mo atoms typically stick, and form a film. The second ion source is operated at low beam energy and moderate current density and directed toward the depositing film to simulate bombardment by plasma ions inside a discharge chamber. This second beam can interact with the depositing film in several ways. If it is too intense, the depositing film can be sputtered away.

This dual source configuration: that of a depositing film being lightly bombarded with ions during the deposition, is a reasonable approximation to the conditions on certain components inside an ion thruster. By changing the rate of deposition, or the energy and flux of the bombarding ions from the second ion source on the film, it is possible to simulate film growth under various thruster operating conditions.

A schematic of the system is shown in Fig. 1. The primary beam is positioned horizontally, and has a moveable faraday cup/shutter. The primary ion source is a 10 cm design, with a 5 cm diameter beam pyrolytic graphite grids. The screen grid apertures were 2.0 mm diameter holes on 2.5 mm centers. The accelerator grid had 1.5 mm diameter holes. The grids were maintained at a spacing of 1.0 mm.

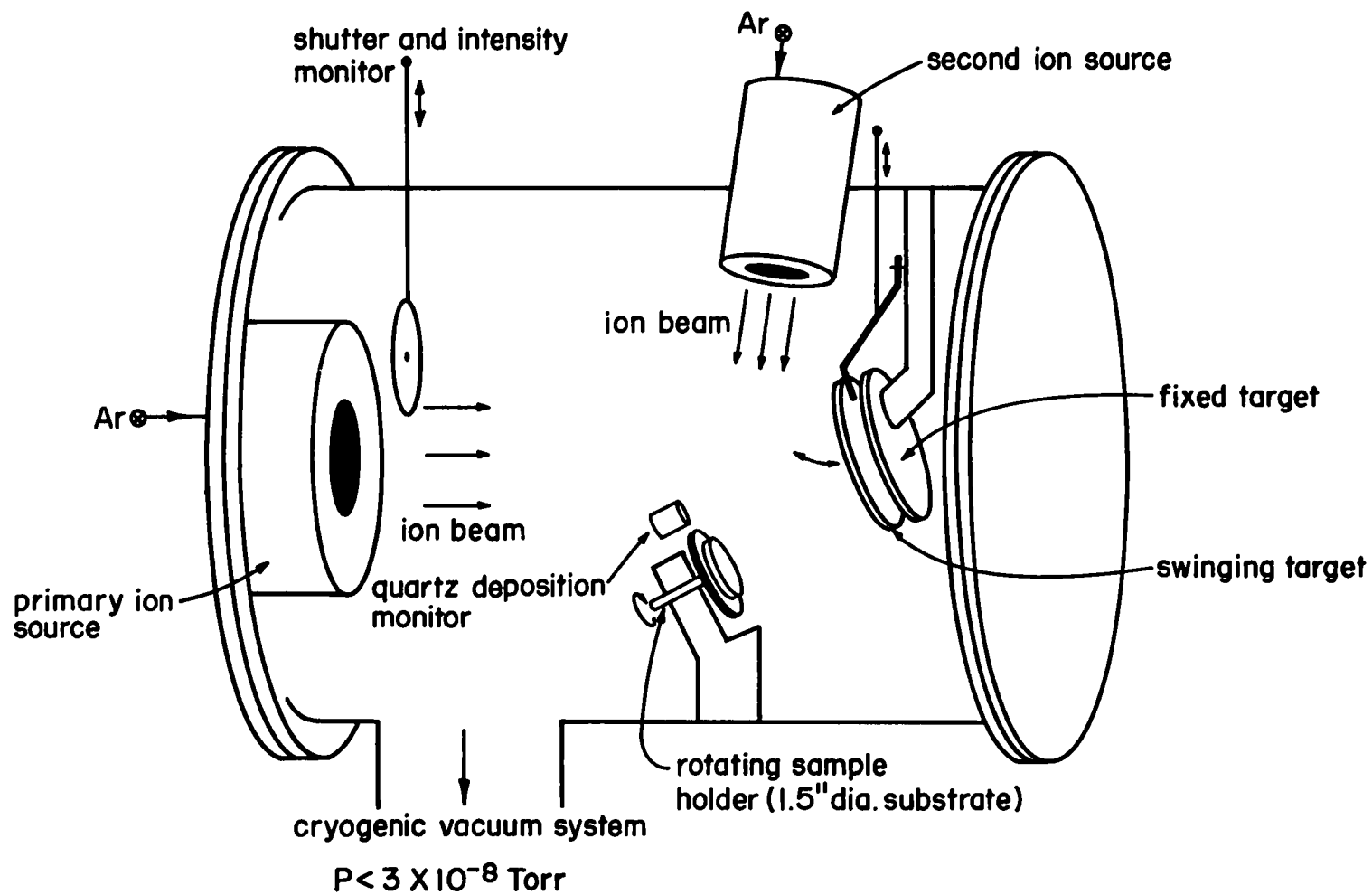


Fig. 1. Schematic diagram of dual ion beam sputtering system.

Neutralization is accomplished using a thermionic Ta filament (not shown). The targets are fixed plates of high purity material. They were water-cooled from the back to avoid warping or melting. The temperature was monitored with a thermocouple. Target temperatures under the most intense conditions (1000 eV, 40 mA ( $2 \text{ mA/cm}^2$ )) were in the  $30^\circ\text{C}$  range. The target materials used for this study were Ta, Mo and Ti.

The second ion source was positioned perpendicular to the primary beam, and pointed down at  $\sim 45^\circ$  angle. The ion source was a multipole type constructed for dual-beam applications. The source had three circular ring anodes on its walls with four accompanying pole pieces. The back plate had no anodes and was flat. The cathode filament was mounted to this back plate. This source had three grids, all of 1 mm graphite. The innermost, or screen grid, had holes of 2 mm diameter on 2.5 mm centers, and was milled to 0.5 mm thickness. The second, or accelerator, grid had 1.25 mm diameter holes. The outermost grid was at ground potential and had 1.45 mm diameter holes. The diameter of the beam was 2.5 cm at the grids. By changing grid potentials, the beam could be focused to 2 cm diameter at a distance of  $\sim 35$  cm, which was the distance to the sample surface. Conversely, the beam could also be broadened significantly at the sample. This had the effect of varying the ion current density at the sample. The 2.5 cm ion source has a maximum current density capability of about  $0.8 \text{ mA/cm}^2$  at 500 eV at the source, limited by the range of available power supplies. Typical current density values at the sample, however, were maintained in the  $0.1$  to  $0.01 \text{ mA/cm}^2$  range, to avoid removing the depositing atoms faster than they were arriving.

The sample holder went through several iterations before arriving at the final design. Because the focusing of a three-grid source is very sensitive to beam and accelerator voltages, it was found necessary to include two Faraday detectors in the sample holder. These were positioned symmetrically with two sample locations to give a good measure of the arriving ion current density at the sample. Due to the long (35 cm) source-to-sample distance, significant charge exchange was probably occurring. Using earlier calculations,<sup>19</sup> for beams in the range of 100 to 300 eV, a mean-free path for charge exchange at  $10^{-4}$  Torr is estimated at about 100 to 120 cm. Measuring the current 35 cm away at the sample leads to an underestimation of the arriving energetic flux by  $\sim$  25-30%. While this feature should be kept in mind for calculation of the actual flux yielding a certain film stress condition, it is not crucial to observation of the general trends. The reported values in this report will be the measured values without this correction.

Samples were generally of two types: thin glass disks and small silicon (100 orientation) chips. The glass disks were used in stress analysis, to be described below. The silicon samples were used primarily for Auger Electron Spectroscopy analysis, for adhesion testing, and also thickness measurements using the Talysurf and the Angstrometer.

All of these simulations were run using argon in both the primary and secondary beams. While, in principle, other gases are often present, there were no attempts to introduce particular gases, such as  $N_2$  or  $O_2$ , to affect film properties.

This dual ion source system was situated in a stainless steel vacuum system of 14 cm diameter by 30 cm length. The system was pumped

with a closed-cycle liquid He cryopump, and had a base pressure of  
 $\sim 1 \times 10^{-7}$  Torr with no gas flow.

## IV. STRESS AND ITS MEASUREMENT IN FILMS

Deposited films are often in a state of stress. This stress is of two forms, compressive and tensile. The first is where the film has a tendency to enlarge slightly, but is being prevented from doing so by its adhesion to the substrate. This type of stress is known as compressive stress, and is by convention assigned a negative value. Conversely, if the film has a tendency to contract, but is constrained by adhesion to the bulk, the stress is positive. This is called tensile stress. Stresses in films are often caused by a mismatch in thermal expansion coefficients. Changing the temperature from the temperature at the time of deposition leads to stress of this type, as the film and the substrate change their dimensions unequally. This is a serious problem with certain materials, such as Pb or Ag, used in specific applications, such as cryogenic microelectronics. It is, however, not expected to be a dominant problem with thruster-related films. Intrinsic film stress often results from the deposition process alone. Intrinsic stresses result when the film material is in a different atomic arrangement from its normal, bulk configuration. This is usually observed as a slightly modified lattice spacing. This modification can result when the film is deposited incrementally, i.e., the film is never thermodynamically near its melting point and never has an opportunity to crystallize. Atoms are added randomly to this growing film, and the resultant lattice spacing is different from the bulk.

The type of deposition process has some effect on the film properties. Sputter-deposited films are often in an intrinsic compressive stress condition because of the presence of many interstitial atoms due to the relatively high arrival energy of sputtered atoms.

Evaporated films are often in tensile stress. The sample temperature during deposition can also be an important factor to intrinsic stress. However, there are no general trends as to its effect.

Film stress is an important parameter in thin film properties. If the stress in the film becomes large enough, it will exceed the adhesion of the film-substrate interface and the film will peel off. Compressive stress failure is often in the form of buckling or bubbling, as seen in Fig. 2. It is this stress-induced failure of a thin film which is relevant to long-term thruster operation. If the formation of thin films in a thruster cannot be prevented, then reducing their stress and/or increasing their adhesion would be desirable. As long as the film adhesion is strong enough to keep the film from buckling under stress, the film will not fail.

The stress in a film on a thin circular substrate can be calculated as<sup>20</sup>

$$S = \frac{Ed^2}{6(1-D)t} (1/R - 1/R_0)$$

where  $E$  is the substrate's Young's modulus,  $d$  is the substrate thickness,  $D$  is Poisson's ratio for the substrate,  $t$  is the film thickness, and  $R_0$  is the initial radius of curvature (if any) for the disk.  $R$  is then the observed radius of curvature of the disk after the film has been deposited.

Measuring the stress in a film is accomplished in a variety of ways. Usually the film is deposited on a very thin substrate. This substrate then distorts because of the force of the stress. Measuring the distortion is a measure of the stress. This is done with long, narrow substrates fixed at one end,<sup>21</sup> or with circular glass disks. These bowed

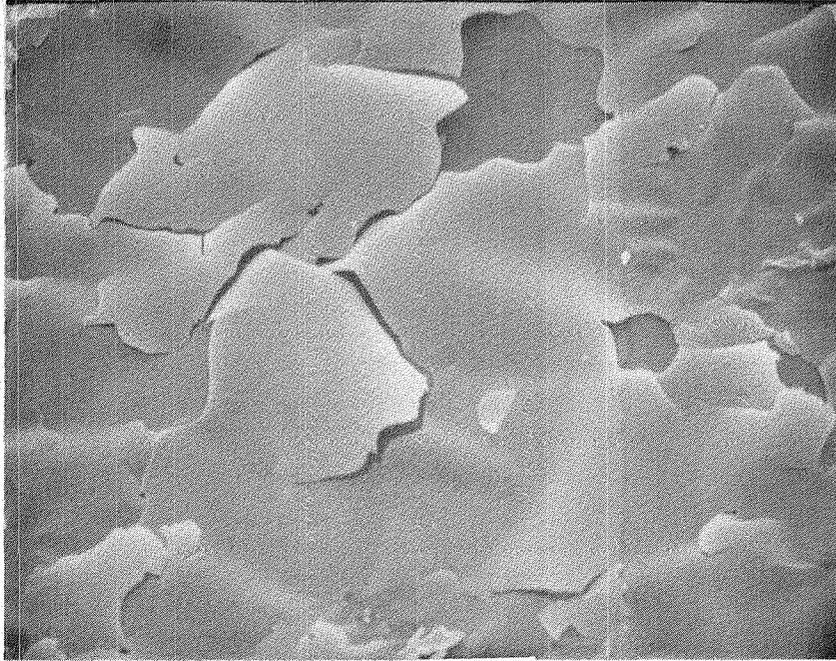


Fig. 2. Mo film failing due to compressive stress (300x). Film deposited near grid area in 15 cm thruster; run time 8 hours.

glass disks are then measured in a Newton's Rings device. The bow of the disk can also be measured with a physical profiling device, such as a Talysurf. An additional measure of the stress can be made by actually measuring the lattice spacings in the film by means of x-ray diffraction. The measured lattice spacings can then be compared with bulk values, and the stress calculated.

Each of these methods has certain advantages. However, many of them require specialized substrates or else long periods of time for measurement. We have developed a much simpler, faster method to measure stress. This method utilizes geometrical optics. In this method, thin glass disks are used as substrates. Usually microscope cover slips (18 mm diameter, 0.2 mm thick) are used, which are readily available and inexpensive. The method uses the feature that the films distort the substrate into a paraboloid shape, or, to first approximation, a sphere. The focal length of this spherical mirror can easily be measured by simple geometrical optics. The radius of curvature is then easily obtained, and with some knowledge of the physical properties of the glass, the stress can be calculated. The results have been quite repeatable, and compare within a few percent to other methods. The primary advantage of this method, aside from inexpensive substrates, is ease and speed of measurement. A simple device has been constructed using a small laser and an arrangement of lenses and mirrors as shown in Fig. 3. Measurements typically take 15 to 30 seconds, and the accuracy is comparable to other methods. A description of this method has been published previously<sup>22</sup> and is included as an appendix.

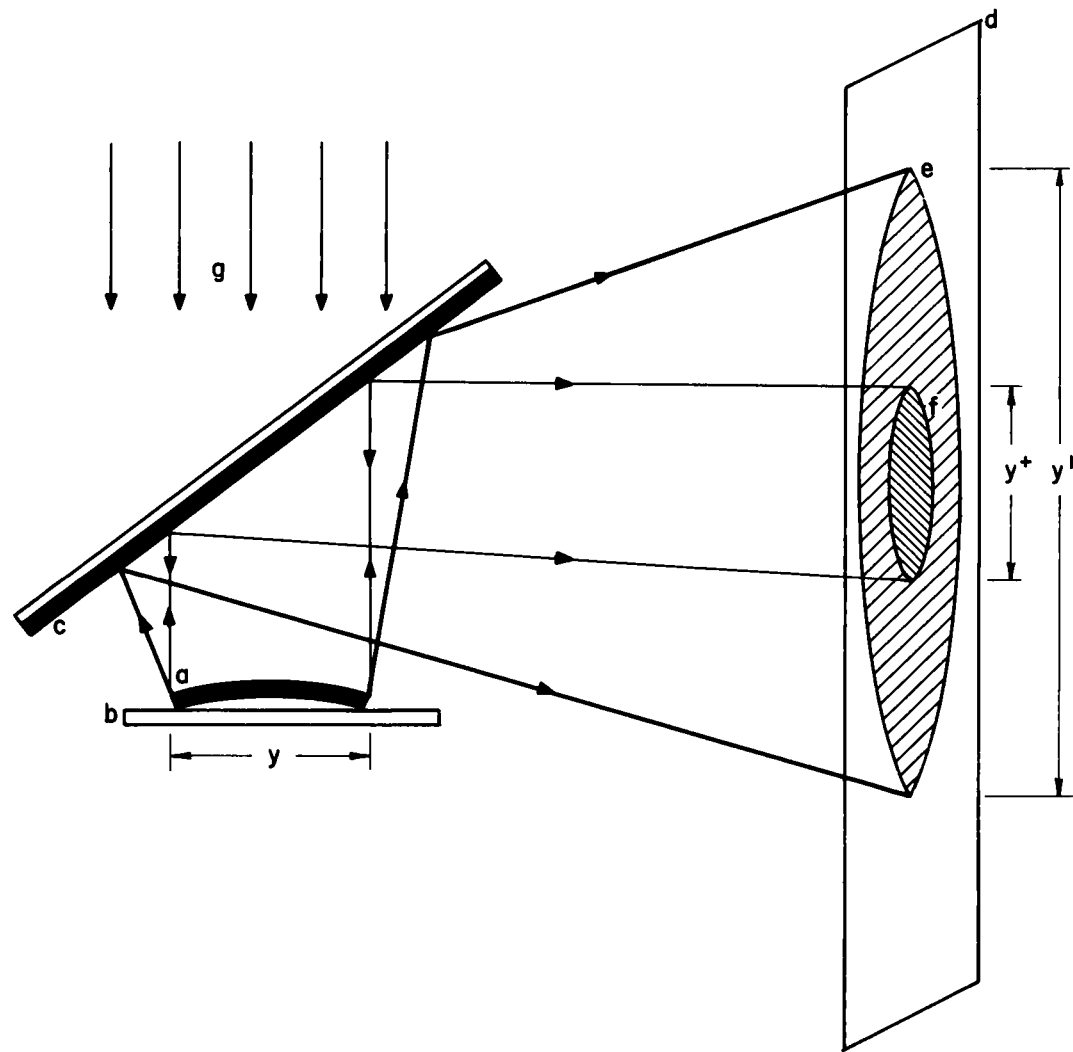


Fig. 3. Schematic of sample stress measurement apparatus. (a) Sample disk; (b) lightly silvered mirror; (c) half-silvered mirror; (d) screen; (e) image of bowed disk; (f) shadow of disk; and (g) incoming parallel light source. In this case,  $y = y^+$ .

## V. PROCEDURE AND RESULTS

The results from the thruster simulations and from the dual beam system will be discussed separately. Then any implications of these results will be discussed.

### A. Films Inside a Thruster

As mentioned above, samples of various types were placed at different positions inside the 15 cm thruster. The thruster was then operated for significant lengths of time under various operating conditions, and the samples removed and analyzed. The primary locations for samples were: the back plate of the source (which is at cathode potential); attached to one of the ring anodes, generally on the sides near the tip; on the magnetic pole pieces; and on the discharge chamber wall adjacent to the grids. The samples were either pieces of polished, doped silicon ( $\sim 1 \text{ cm}^2$ ) which can be treated as being at the same potential as the surface to which they were attached, and small thin glass disks, whose surface can be considered to be at floating potential. These thin glass disks were used as substrates for film stress measurements.

Two discharge parameters were individually varied, and the resultant effect on the depositing films determined.

Primary among these was the discharge voltage, which translated into a variation of the ion and electron energy. This discharge voltage ranged from 35 V which will be designated "low" to 80 V, which will be designated "high". The other parameter which was varied was the discharge current, from a low of 0.5 A to a maximum of 3.5 A. Usually the length of time of thruster operation was varied inversely with the discharge current at a constant voltage, to give a constant effective "dose" to the walls.

After the initial operation of the ion source at 40 eV discharge, films were found to be deposited on the flat, upstream end, the cylindrical walls, the anodes, and the wall area near the grids. Typically the films were smooth except for this latter area near the grids. Here the films failed and peeled. Analysis with a Scanning Electron Microscope (SEM) showed evidence of compressive stress failure (see Fig. 2). The rate of deposition for most areas was  $\sim 80 \text{ \AA}$  per hour of operation. This would translate into a  $1 \mu$  thick film in approximately 125 hours of operation. This deposition rate would correspond to an  $80 \mu$  film deposited in a mission time of  $10^4$  hours which would undoubtedly fail. The composition of films from these and numerous other runs was measured by AES, and depth profiles taken. The films were typically composed of Ta, Mo, C, Fe, and O. Depth profiles showed the O to be mainly a surface contaminant (Fig. 4). This leaves the bulk of the film to be Ta, C, Mo, and Fe. The films near the grids were much higher in Mo concentration.

The source of most of these species can be traced. The Ta is from the hot filament cathode, which is slowly evaporating as well as being heavily sputtered by the discharge ions. The Mo is from the dished grids, and the higher levels in the films near the grids are not surprising. The presence of the C is indicative of contamination of the system, probably by diffusion pump oil. The Fe is probably from exposed magnets and pole pieces which are all at the same potential.

The Ta, being from the hot filament cathode, represents a departure from the idealized simulation of a thruster. This is due to the feature that long term operation will necessitate hollow cathode operation inside the chamber. The stress in films deposited at the back plate of

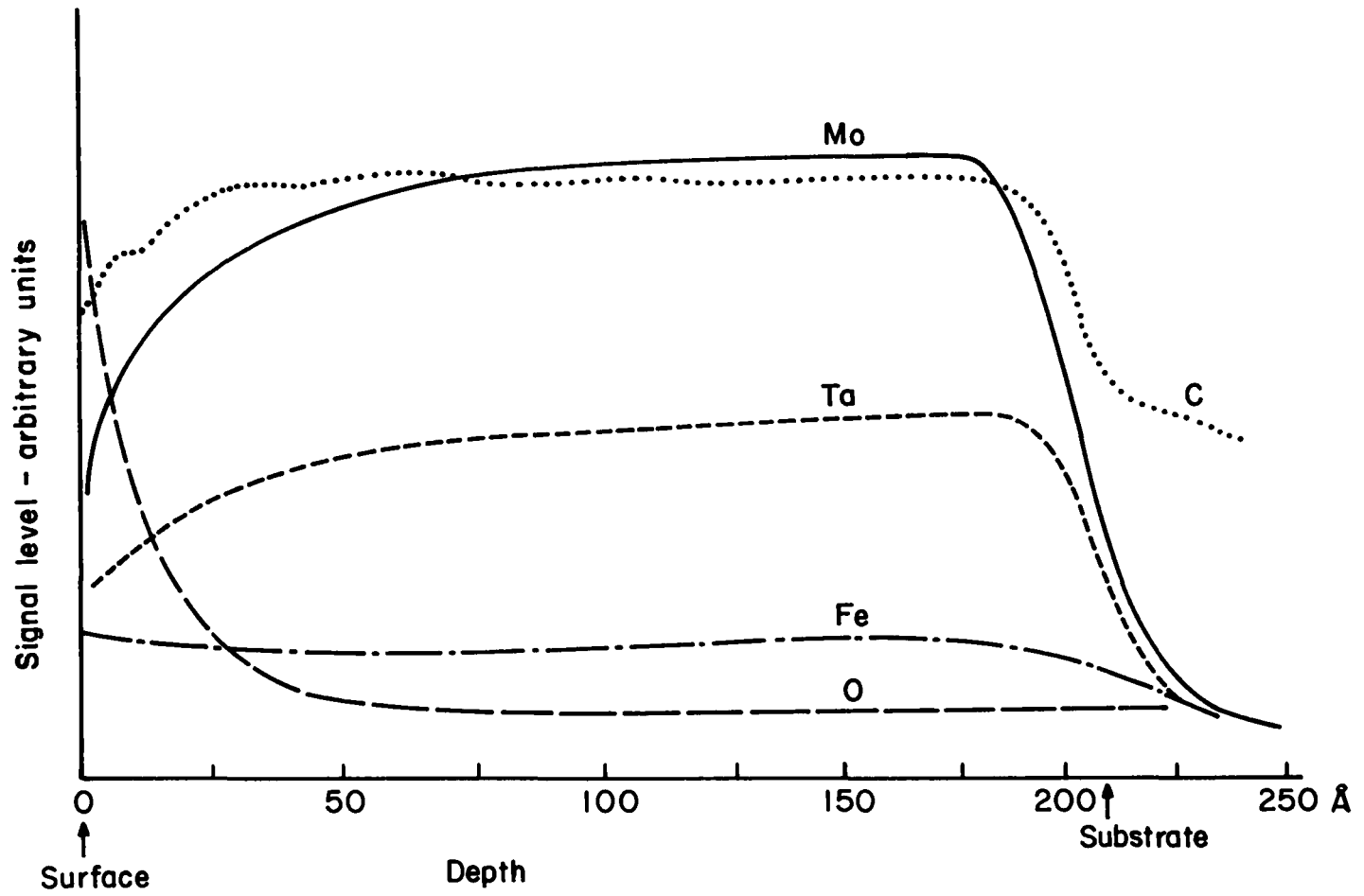


Fig. 4. Sample AES depth profile of deposited film.

the thruster was always compressive, which is characteristic of sputter-deposited films.

Stresses in films deposited near the grids were in the  $3-6 \times 10^9$  dynes/cm<sup>2</sup> range for similar film thicknesses, and were very consistent under similar discharge conditions.

Upon operating the thruster at high discharge voltage but the same discharge current, a marked change in the characteristics of the deposited films was noted. The films were thinner; the deposition rate was only  $\approx 20 \text{ \AA}$  per hour of operation. However, the films were not metallic, and in fact, at the highest discharge voltages, the films were almost transparent. This is indicative of the presence of oxygen in the films. Auger analysis confirmed high oxygen and carbon levels and reduced metallic components. The presence of these oxide films indicates the existence of an oxygen supply, probably in the form of an air leak into the chamber. These films were deposited on glass substrates which would tend to reach a floating potential somewhere intermediate of the cathode and anode potentials. It is possible that at the higher discharge voltages, the potential difference between the substrate and plasma potential was sufficient to significantly exceed the sputtering threshold and result in removal of material almost as fast as it was being deposited. It is also possible that oxygen levels increased systematically as more tests were performed, thus reducing the sputtering rate of interior surfaces. It would appear that O<sub>2</sub> was probably present at all times in the thruster. This is, again, not totally in keeping with the object of the experiment, that of simulating space-type thrusters. The marked reduction in film growth rate, however, may be a useful feature.

The stress in these high-discharge-voltage films was slightly below that of the low discharge voltage, metallic deposits. This is somewhat misleading due to the large difference in film thickness. For equal thickness films, the high-discharge voltage, somewhat dielectric films, are in much higher stress than the low discharge voltage films.

Following several hundred hours of discharge operation with the ion source under a variety of conditions, the ion source was disassembled to observe the location and condition of films on the actual thruster parts. The pole pieces were the only parts that appeared not to have any heavy film deposited on them. They appeared to have been slightly etched, although this may be due to a thin light colored film. The back plate of the ion source was heavily deposited with a thick gray film. There was no evidence of failure, even though the film was several microns thick. This area was in direct contact with discharge plasma and the films were relatively rich in Ta compared to films further downstream.

The ring anodes showed evidence of film deposition as well as film failure. However, there was a difference between the "top" side of the anode and the side facing the back plate. The top sides, which faced the screen grid, were heavily flaked and peeled. The bottom surface, while coated by a thick film, showed no adhesion failure or peeling. Film thickness in each case was several microns. As will be discussed later, this peeling on the side exposed to the grids can be traced to high Mo levels; the Mo being sputtered from the grids. The other area which showed strong evidence of film deposition and failure was on the cylindrical side walls of the chamber. These walls were located behind the anodes and pole pieces. The films were several microns thick, and

failed due to high compressive stress. This was evident by the buckling mode of failure. These films could not be analyzed because appropriate removable substrates could not be mounted here. They were metallic, and mildly magnetic, which suggests a high Fe concentration possibly from the pole pieces. The films on the wall area near the grids also peeled heavily, but these flakes were nonmagnetic. This suggests, again, a high Mo level.

#### B. Film Formation in a Dual Ion Beam System

The dual ion beam system described above was used to deposit films of thruster-type materials under conditions that could approximate the conditions inside a thruster discharge chamber. The films used for these simulations were pure film of Ta, Mo and Ti. Stainless steel was not used because it is a complex alloy, and it was suspected that small amounts of impurities might affect film properties. The use of pure materials in this part of the experiment was intended to simplify interpretation of the results. Time did not permit continuation into the study of alloy films of the type that are deposited in ion thrusters. The films were all sputter-deposited using a primary sputtering beam of 1000 eV Ar<sup>+</sup>. The energy of this primary beam has almost no effect on the energy distribution of the sputtered material,<sup>23</sup> so there should be no significant energy difference between these sputtered atoms and those sputtered by much lower energy ions in the thruster discharge chamber. The deposition rate, however, greatly exceeded the in-situ thruster deposition rate. Although chemical analyses of these films were not performed, this increased rate would have helped to reduce the relative concentration of background gas contamination in the growing film.

The films were deposited initially without the presence of the second ion beam directed at the target. This was to give some idea of the film stress and adhesion in unperturbed films. Later samples then were bombarded with  $\text{Ar}^+$  ions during the deposition. These ions were varied in energy from 100-500 eV and in current density from 2-100  $\mu\text{A}/\text{cm}^2$ . This allows an ion-to-condensing-atom ratio ranging from  $< 0.01$  to 2 depending on the rate of sputtering of the primary source. The results from each of the materials are given below.

1. Mo:

Films of Mo were in very high stress. The stress ranged upwards of  $6 \times 10^{10}$  dynes/cm<sup>2</sup>. The high stress resulted in substantial film failure for thicker films as the stress exceeded the adhesion. Generally, films greater than 400 Å thick had partial failures, and films thicker than 1000 Å always failed totally. The stress was compressive and the failure mode was always by buckling. The second ion source at energies up to 500 eV and over the entire current density range had no effect in film stress or adhesion.

2. Ta:

Films of Ta were substantially lower stress than Mo films. Stresses were compressive, and in the  $6-8 \times 10^9$  dynes/cm<sup>2</sup> range. The films showed no obvious signs of peeling up to  $\sim 10,000$  Å in thickness. Again, however, the second ion source over its entire energy and current density range had no effect on the film properties.

3. Ti:

Ti films were in even lower stress than the Ta or Mo films. Values compressive stress in the  $2-3 \times 10^9$  dynes/cm<sup>2</sup> range were obtained in the absence of secondary beam bombardment. No evidence of failure was observed for films up to 1  $\mu$  in thickness. The effect of

the second ion beam, however, was to increase the stress in the film as a function of increasing ion bombardment energy as shown in Fig. 5. The stress also became more compressive as the ion-to-condensing-atom ratio increased.

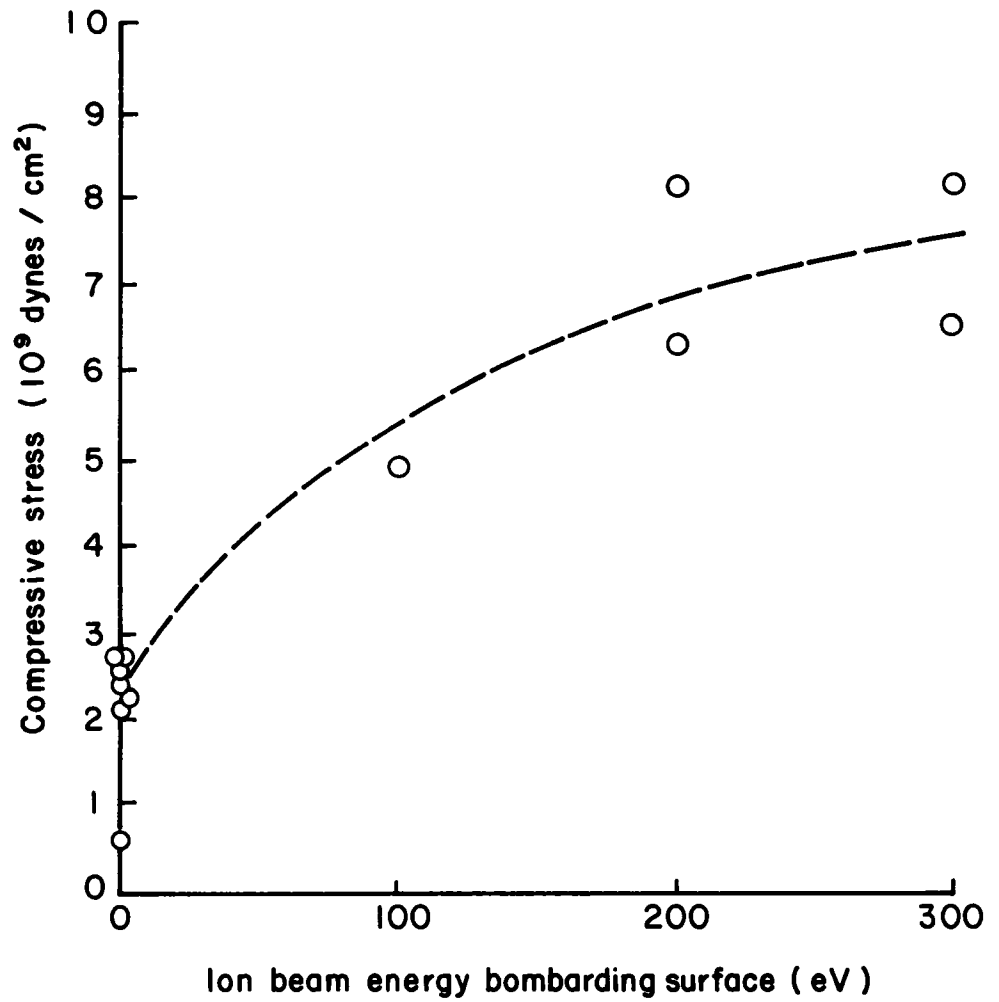


Fig. 5. Ti film stress in dual beam sputtering configuration as a function of secondary bombarding ion beam energy.

## VI. CONCLUSIONS

This work has concentrated in two areas. The first has been to operate thrusters for multi-hour periods and to observe and measure the films found inside the thruster. The second has been to simulate the environment inside the discharge chamber of the thruster by means of a dual ion beam system. Here, films were sputter deposited in the presence of a second low energy bombarding beam to simulate film deposition on thruster interior surfaces that undergo simultaneous sputtering and deposition.

A few conclusions can be reached from this two-part study. One conclusion is that Mo in particular presents serious problems for use in a thruster as far as film deposition is concerned. Mo films were found to be in high stress, making them more likely to peel and flake. The effect of ion bombardment on the properties of these Mo films was negligible. Of the two other materials, Ta and Ti, Ta seems to have more desirable film properties for thruster applications. Although the Ta film properties were not modified due to ion bombardment in the dual ion beam deposition experiments. Titanium is originally in lower stress than Ta or Mo; the observed increase of stress with bombardment energy suggests that inside a thruster, the stress of this material would possibly be higher but probably not as great as Ta or Mo.

The thruster discharge chamber tests showed the expected substantial deposition and peeling problems with long operating times. Some films of relatively high Ta levels in the ion thruster that were heavily bombarded showed no failure at thicknesses of several microns. The tests with increased discharge voltage were inconclusive because the nature of the film changed as well as the rate of deposit at the

higher voltages. The film properties for these films were governed more by the reactive gases inadvertently present in small quantity than by processes comparable to operation on a spacecraft.

## REFERENCES

1. Kaufman, H. R., "An Ion Rocket with an Electron-Bombardment Ion Source," NASA TN-D-585, Jan. 1961.
2. Lewis Research Center, "30-Centimeter Ion Thrust Subsystem Design Manual," NASA TM-79191, June 1979.
3. TRW Defense and Space Systems Group, "8 cm Mercury Ion Thruster Subsystem Users Manual," July 1977.
4. Beattie, J. R., "A Model for Predicting the Wearout Lifetime of the LeRC/Hughes 30-cm Mercury Ion Thruster," AIAA Paper No. 79-2079, 1979.
5. Kerslake, W. R., R. G. Goldman, and W. C. Nieberding, "SERT II: Mission, Thruster Performance and In-Flight Thrust Measurements," J. Spacecr. Roc., Vol. 8, No. 3, pp. 213-224, March 1971.
6. Ion Physics Department Staff, Hughes Research Laboratories, "Thruster Endurance Test," NASA CR-135011, May 1976.
7. Ion Physics Department Staff, Hughes Research Laboratories, "Fabrication and Verification Testing of ETM 30-cm Diameter Ion Thrusters," NASA CR-135193, April 1977.
8. Power, J. L., "Accelerated Life Test of Sputtering and Anode Deposit Spalling in a Small Mercury Ion Thruster," NASA TMX-3269, September 1975.
9. Power, J. L. and D. J. Hiznay, "Solutions for Discharge Chamber Sputtering and Anode Deposit Spalling in Small Mercury Ion Thrusters," AIAA Paper No. 75-399, March 1975.
10. Manteniaks, M. A. and V. K. Rawlin, "Sputtering Phenomena of Discharge Chamber Components in a 30-cm Diameter Hg Ion Thruster," AIAA Paper No. 76-988, November 1976.
11. Beebe, D. D., S. Nakanishi, and R. C. Finke, "Electric Arc Discharge Damage to Ion Thruster Grids," NASA TM X-3044, May 1974.
12. Rawlin, V. K. and M. A. Manteniaks, "Effect of Facility Background Gases on Internal Erosion of the 30-cm Hg Ion Thruster," AIAA Paper No. 78-665, NASA TM-73803, April 1978.
13. Wilbur, P. J., "A Model for Nitrogen Chemisorption in Ion Thrusters," AIAA Paper No. 79-2062, 1979.
14. Masaki, S., "Sputtering Rates of Discharge Chamber Materials," in NASA CR-165253, pp. 53-67, December 1980.
15. Hirsch, E. H. and J. K. Varga, "The Effect of Ion Irradiation on the Adherence of Germanium Films," Thin Sol. Films, Vol. 52, pp. 445-452, 1978.

16. Franks, J., P. R. Stuart and R. B. Withers, "Ion Enhanced Film Bonding," Thin Sol. Films, Vol. 60, pp. 231-236 (1979).
17. Harper, J. M. E., IBM Thomas J. Watson Research Center, private communication.
18. Hoffman, D. W. and J. A. Thornton, ""Effects of Substrate Orientation and Rotation on Internal Stresses in Sputtered Metal Films," J. Vac. Sci. Technol., Vol. 16(2), pp. 134-137, March/April 1979.
19. Robinson, Raymond S., Ph.D. Thesis, Colorado State University.
20. Thornton, J. A., J. Tabock and D. W. Hoffman, Thin Solid Films, Vol. 64, p. 111, 1975.
21. Cambell, D. S., in Handbook of Thin Film Technology, L. T. Maissel and R. Glang, eds., (McGraw Hill, New York, 1970), pp. 12-30.
22. Rossnagel, S. M., P. Gilstrap and R. Rujkorakarn, "Stress Measurement in Thin Films by Geometrical Optics," J. Vac. Sci. Technol., Vol. 21(4), pp. 1045-1046, 1982.
23. Wehner, G. K. and G. S. Anderson, in Handbook of Thin Film Technology, L. I. Maissel and R. Glang Eds., McGraw Hill, pp. 3-20, 1970.

## Stress measurement in thin films by geometrical optics

S M Rossnagel, P Gilstrap, and R Rujkorakarn

*Department of Physics, Colorado State University, Fort Collins, Colorado 80523*

(Received 8 June 1982, accepted 28 July 1982)

### I. INTRODUCTION

The stress in a thin film on a bulk substrate is an important factor relating to the film's adhesion and behavior under temperature variation. Generally, methods of measuring stress are complicated. Most begin with depositing films on very thin substrates, which then deform under the film's stress. The deformation can be measured with light interference patterns (Newton's rings),<sup>1</sup> by physical displacement of the substrate as in a beam bending device,<sup>2</sup> or by measuring the "bow" of substrate either with a Talysurf-like device<sup>3</sup> or a light microscope.<sup>4</sup> Other methods involve x-ray diffraction<sup>5</sup> to measure actual atomic displacement. Most of these methods are complicated and often require long periods of time to complete or entail very specialized substrates—as in the beam-bending or Newton's rings device.

We propose a simple variation of the Newton's rings experiment for quick, relatively accurate stress measurements. The method involves depositing a thin film on a small circular thin substrate, in this case a common microscope cover slip (18 mm diam  $\times$  0.18 mm). The thin film then deforms the coverslip into roughly a paraboloid shape. However, instead of using the interference of light between this sample and an optical flat, as in the Newton's rings experiment, the focal length of this "spherical mirror" is determined optical-

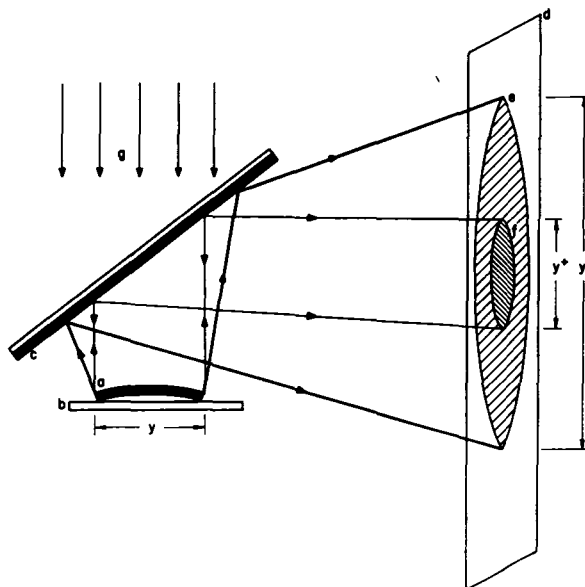


FIG 1 Schematic of geometrical optics technique (a) sample disk, (b) lightly silvered mirror; (c) half-silvered mirror, (d) screen, (e) image of bowed disk, (f) shadow of disk, and (g) incoming parallel light source. In this case,  $y = y'$ .

TABLE I Radii of curvature for five different samples by Talysurf method, geometrical optics method, and Newton's rings method

Sample	Talysurf	Radius of curvature		Stress Geometrical optics (only)
		Geometrical optics	Newton's rings	
1 1100 Å Mo	1.21 m	1.26 m	1.14 m	$-3.7 \times 10^{10}$
2 600 Å Mo	2.06 9.8,	2.16 9.5,	1.96 16.5,	$-3.9 \times 10^{10}$ $+7.2 \times 10^{10}$
3 750 Å Al	35* 6.0,	31.8* 5.95,	37.2*	$+2.1 \times 10^9$ $+2.9 \times 10^9$
4 2963 Å Al	13*	15.0*		$+1.1 \times 10^9$
5 3440 Å Ta	1.7	1.83	1.52	$-8.2 \times 10^9$

\*x and y directions on nonuniformly bowed samples

ly by reflecting parallel light from its surface onto a screen. Any magnification or contraction of the image of the film is indicative of distortion of the substrate due to film stress. Such magnification, whether greater or less than one, immediately determines the sign of the stress. From Fig. 1, the radius of curvature of the disk can be found as

$$R = \frac{2yD}{y' - y}$$

where  $y$  is the diameter of the sample,  $y'$  is the diameter of the image of the sample, and  $D$  is the path length from the sample to the screen. This arrangement has proved to be slightly unwieldy for two reasons: first, because the samples are small (18 mm diam), small changes in size are difficult to measure, and second, though expanding a 1-mm-diam laser beam to  $\sim 25$  mm is theoretically trivial, in practice it is often difficult or expensive. For that reason, we have changed Fig. 1 to use a slightly diverging beam. This changes the above relation to

$$R = y / [2 \tan\{\frac{1}{2} \text{atn}[(y' - y)/2D]\} - \frac{1}{2} \text{atn}[(y' + y)/2D]] \\ \approx \frac{2yD}{y' - y^+}$$

where  $y^+$  is the diameter of the image of the unbowed disk (the shadow in Fig. 1).

The stress is then calculated from the radius of curvature by standard means<sup>6</sup>

$$S = \frac{Ed^2}{6(1 - \nu)t} (1/R - 1/R_0)$$

where  $t$  is the film thickness,  $E$ ,  $d$ ,  $\nu$ , and  $R_0$  are the substrate's Young's modulus, thickness, Poisson's ratio, and initial (if any) radius of curvature, respectively.

## II. RESULTS

The above method has been used to measure the radius of curvature for a series of film depositions with Ta, Al, and Mo films. The radii were also measured by the Newton's rings method and the Talysurf method. The results are shown in Table I.

The results of these three methods are in reasonably good agreement over a large range of radii of curvature. The geometrical optics method has sensitivity in the  $1 \times 10^9$ -dyn/cm<sup>2</sup> range (although this number is directly dependent on film thickness), which corresponds to the practical radius limit of  $\sim 50$  m and for the Newton's rings (one fringe) is  $\sim 125$  m. The repeatability of the geometrical optics method is good, usually within 5%. It also easily shows asymmetries in the bowing of the disk.

Finally, an important feature in each of these measurements is the time involved. The Talysurf method has a long set-up period. The measurement typically takes 30–40 min. The Newton's rings method can take a similar time, although with sufficient practice (particularly in getting the sample correctly placed), this might be reduced to 5–10 min. The geometrical optics method typically takes 1/2–1 min.

## III. CONCLUSION

This method described for measuring stresses in film is simple, fast, and inexpensive, requiring only a laser, mirrors, and a diverging lens. The stresses measured are in reasonable agreement with other methods requiring substantially more time and effort. The method also allows the use of cheap substrates with relatively low optical qualities.

*Acknowledgments* The authors would like to thank J. R. Sites and R. S. Robinson for their helpful discussions. This work was supported under grants from NASA Grant NAG 3-209 and Air Force Weapons Laboratory Contract F-29601-82-K-0009.

<sup>1</sup>J. D. Finegan and R. W. Hoffman, *Trans. 8th Vacuum Symposium and Second Int'l Congress* (MacMillan, New York, 1962), p. 935.

<sup>2</sup>D. S. Cambell, *Trans. 9th Nat'l Vacuum Symp.* (MacMillan, New York, 1962), p. 29.

<sup>3</sup>P. Gilstrap (private communication).

<sup>4</sup>R. Glang, R. A. Holmwood, and R. L. Rosenfeld, *Rev. Sci. Instrum.* **36**, 7 (1965).

<sup>5</sup>D. S. Cambell, in *Handbook of Thin Film Technology*, edited by L. I. Maissel and R. Glang (McGraw-Hill, New York, 1970), pp. 12–30.

<sup>6</sup>J. A. Thornton, J. Tabock, and D. W. Hoffman, *Thin Solid Films* **64**, 111 (1975).

1 Report No NASA CR-168172		2 Government Accession No		3 Recipient's Catalog No	
4 Title and Subtitle Sputtering Phenomena in Ion Thrusters				5 Report Date February 1983	
				6 Performing Organization Code	
7 Author(s) Raymond S. Robinson and Stephen M. Rossnagel				8 Performing Organization Report No	
9 Performing Organization Name and Address Physics Department Colorado State University Fort Collins, CO 80521				10 Work Unit No	
				11 Contract or Grant No Grant NAG 3-209	
12 Sponsoring Agency Name and Address NASA Lewis Research Center 21000 Brookpark Road Cleveland, OH 44135				13 Type of Report and Period Covered Contract Report 1 year	
				14 Sponsoring Agency Code	
15 Supplementary Notes Grant Manager, Maris A. Mantenleiks NASA Lewis Research Center 21000 Brookpark Road Cleveland, OH 44135					
16 Abstract  Sputtering effects in discharge chambers of ion thrusters can be lifetime limiting in basically two ways. (1) ion bombardment of critical thruster components at energies sufficient to cause sputtering can remove significant quantities of material; enough to degrade operation through adverse dimensional changes or possibly lead to complete component failure, and (2) metals sputtered from these intensely bombarded components can be deposited in other locations as thin films and subsequently flake or peel off; the flakes then lodging elsewhere in the discharge chamber with the possibility of providing conductive paths for short circuiting of thruster components such as the ion optics.  This experimental work has concentrated in two areas. The first has been to operate thrusters for multi-hour periods and to observe and measure the films found inside the thruster. The second has been to simulate the environment inside the discharge chamber of the thruster by means of a dual ion beam system. Here, films were sputter deposited in the presence of a second low energy bombarding beam to simulate film deposition on thruster interior surfaces that undergo simultaneous sputtering and deposition. Mo presents serious problems for use in a thruster as far as film deposition is concerned. Mo films were found to be in high stress, making them more likely to peel and flake. The effect of ion bombardment on the properties of these Mo films was negligible. Of the two other materials tested systematically, Ta and Ti, Ta seems to have more desirable film properties for thruster applications. Thruster discharge chamber tests showed the expected substantial deposition and peeling problems with long operating times. Some films of relatively high Ta levels in the ion thruster that were heavily bombarded showed no failure at thicknesses of several microns.					
17 Key Words (Suggested by Author(s)) Ion Ion Thruster Sputtering Stress in Films Thin Films Electric Propulsion			18 Distribution Statement  Unclassified, unlimited		
19 Security Classif (of this report) Unclassified		20 Security Classif (of this page) Unclassified		21 No of Pages 33	22 Price*

\* For sale by the National Technical Information Service, Springfield, Virginia 22161

**End of Document**